Transmittance of Gaussian beams in biological tissues

Özcan, Murat Kaan; Gökçe, Muhsin Caner; Baykal, Yahya

DOI
10.1016/j.jqsrt.2024.109312

Publication date
2024

Document Version
Final published version

Published in
Journal of Quantitative Spectroscopy and Radiative Transfer

Journal of Quantitative Spectroscopy & Radiative Transfer 333 (2025) 109312

Contents lists available at ScienceDirect

Journal of Quantitative Spectroscopy and Radiative Transfer

journal homepage: www.elsevier.com/locate/jqsrt

Transmittance of Gaussian beams in biological tissues

Murat Kaan Özcan [a], Muhsin Caner Gökçe [b,c,*], Yahya Baykal [a]

[a] Çankaya University, Department of Electrical-Electronics Engineering, Yukarıyurtçu Mah. Mimar Sinan Cad. No: 4, Etimesgut, 06790, Ankara, Turkey
[b] TED University, Department of Electrical and Electronics Engineering, 06420 Kolej Çankaya, Ankara, Turkey
[c] Delft University of Technology, Department of Geoscience and Remote Sensing, 2628 CD Delft, The Netherlands

ARTICLE INFO

Keywords:
Biological tissue
Optical wave propagation
Average intensity
Tissue turbulence
Absorption, Scattering
Transmittance

ABSTRACT

The study examines the average transmittance of Gaussian beams passing through various biological tissues, taking into account the impact of turbulence, absorption, and scattering. The extended Huygens-Fresnel technique, which utilizes the power spectrum of turbulent biological tissues, is applied to determine the optical intensity at the observation point. Additionally, there are tabulated absorption and scattering coefficients available for the application of the Beer-Lambert law, facilitating the calculation of optical light attenuation in biological tissues. Examining the impact of turbulence, as well as absorption and scattering-induced attenuation on the Gaussian beam's propagation, the changes in transmittance are documented across different tissue parameters.

1. Introduction

Studying the propagation characteristics of a light beam through biological tissue, which encompasses aspects like intensity profile, effective beam spot radius, spectral degree of coherence, polarization, scintillation and average transmittance, provides valuable insights into the internal structures of the tissue medium. The propagation of light through biological tissue is impacted by factors such as absorption, scattering, and turbulence. As light traverses through the tissue, it undergoes scattering and absorption, leading to a reduction in light intensity known as attenuation. Studies in the literature have documented the absorption and scattering coefficients for diverse tissue types [1–5]. Furthermore, the turbulence within the tissue has a substantial impact on the propagating wave, resulting in various impairments to the wave front. This, in turn, gives rise to phenomena such as beam spread, beam wander, and scintillation. A recent literature survey considering optical wave propagation in tissue turbulence is reported in [6]. Various laser sources respond differently to the influence of tissue turbulence. Refs. [7–12] offer comprehensive details regarding the propagation of various laser sources through turbulent tissue media. Specifically, [7] investigates how tissue turbulence affects the transmission of annular beams, while [8] explores the propagation of laser array beams through liver tissue. In both [7] and [8], the authors present analytical solutions for both received intensity and effective beam spot size. Additionally, [9] scrutinizes the propagation of stochastic electromagnetic vortex beams through turbulent biological tissues, employing the cross-spectral density matrix. The authors in [9] also provide the derived formula for coherence length. An analogous study was conducted to investigate the propagation characteristics of anomalous hollow beams, as detailed in Ref. [10], where the structure constant of the refractive index is expressed in terms of tissue structure parameters. Moreover, [11] delves into the propagation characteristics of coherent Laguerre-Gaussian beams within turbulent biological tissue, whereas [12] details the propagation properties of Generalized Hermite cosh-Gaussian beams through the tissue of the human upper dermis.

The turbulence in the tissue also leads to light scintillation, significantly impairing the effectiveness of optical systems. In recent research studies [13–16], the existence of the scintillation phenomenon has been documented. To elaborate, [13] delves into the scintillation index of an optical spherical wave, [14] provides an analytical expression for the scintillation index of the Gaussian beam wave, [15] offers a comprehensive analysis of the scintillation index for plane, spherical, and Gaussian beam waves in soft biological tissues, and [16] presents analytical solutions for the scintillation index of the Gaussian beam across different turbulence strengths.

This study investigates how a Gaussian laser beam travels through various biological tissues affected by turbulence, absorption, and scattering. Initially, we calculate the average optical intensity at the observation point using the Huygens-Fresnel method, which depends on the turbulence power spectrum of biological tissue. We also account for

* Corresponding author at: TED University, Department of Electrical and Electronics Engineering, 06420 Kolej Çankaya, Ankara, Turkey.
E-mail address: muhsin.gokce@tedu.edu.tr (M.C. Gökçe).

https://doi.org/10.1016/j.jqsrt.2024.109312
Received 19 March 2024; Received in revised form 8 November 2024; Accepted 4 December 2024
Available online 6 December 2024

intensity reduction caused by absorption and scattering using the Beer-Lambert Law. Ultimately, our attention is directed towards understanding the transmittance of the Gaussian beam in biological tissues, taking into account turbulence, absorption, and scattering effects. It is important to highlight that we have utilized tissue parameter data regarding absorption, scattering, and turbulence, which were obtained through empirical measurements from a range of tissue samples.

2. Formulation

2.1. Gaussian beam propagation in tissue turbulence

The field expression of a Gaussian beam at the source plane is formulated as [17]

$$u(\mathbf{s}) = \exp\left(-\frac{\mathbf{s}^2}{2\alpha_s^2}\right) \tag{1}$$

where the vector $\mathbf{s} = (s_x, s_y)$ represents the transverse coordinates of the source on the transmitter plane, and α_s denotes the source size.

Extended Huygens-Fresnel integral dictates the field expression of a Gaussian beam at the receiver plane, accounting for the effects of turbulence experienced by the laser beam over a propagation distance of L [18]

$$u(\mathbf{p}) = \frac{k\exp(jkL)}{2\pi jL}\int_{-\infty}^{\infty}\int_{-\infty}^{\infty} u(\mathbf{s})\exp\left\{\frac{jk}{2L}\left[(s_x-p_x)^2+\left(s_y-p_y\right)^2\right]\right\}\exp[\psi(\mathbf{s},\mathbf{p})]\mathrm{d}s_x\mathrm{d}s_y \tag{2}$$

where $\mathbf{p} = (p_x, p_y)$ is the transverse coordinates of the receiver plane, $k = 2\pi/\lambda$ denotes the wavenumber, λ represents the wavelength of the laser source, $j = \sqrt{-1}$ is the complex number, $\psi(\mathbf{s}, \mathbf{p})$ represents the random complex phase of a spherical wave during its propagation from the source point to the receiver point.

The calculation of the optical intensity at the receiver plane is based on the method outlined in Ref. [18]

$$\begin{aligned}&\langle I(\mathbf{p}, z=L)\rangle = \langle u(\mathbf{p})u^*(\mathbf{p})\rangle\\ &= \left(\frac{k}{2\pi L}\right)^2\int_{-\infty}^{\infty}\int_{-\infty}^{\infty}\mathbf{d}^2\mathbf{s}_1\int_{-\infty}^{\infty}\int_{-\infty}^{\infty}\mathbf{d}^2\mathbf{s}_2 u(\mathbf{s}_1, z=0)u^*(\mathbf{s}_2, \mathrm{z}=0)\\ &\times\exp\left[\frac{ik}{2L}\left(|\mathbf{s}_1-\mathbf{p}|^2-|\mathbf{s}_2-\mathbf{p}|^2\right)\right]\\ &\times\langle\exp[\psi(\mathbf{s}_1,\mathbf{p})]\exp[\psi^*(\mathbf{s}_2,\mathbf{p})]\rangle\end{aligned}, \tag{3}$$

where * represents the complex conjugate and $\langle\rangle$ shows the ensemble average over the random medium statistics. The third line of Eq. (3) is given by [18]

$$\langle\exp[\psi(\mathbf{s}_1,\mathbf{p})+\psi^*(\mathbf{s}_2,\mathbf{p})]\rangle = \exp\left[-\frac{1}{2}D_\psi(\mathbf{s}_1,\mathbf{s}_2)\right], \tag{4}$$

where D_ψ is the wave structure function and is given by

$$D_\psi(\mathbf{s}_1,\mathbf{s}_2) = \frac{2}{\rho_0^2}(\mathbf{s}_1-\mathbf{s}_2)^2. \tag{5}$$

By incorporating Eq. (5) into Eq. (3) and resolving the integral, we arrive at the determination of the optical intensity at the receiver, and this is represented by [19]

$$\begin{aligned}&\langle I(\mathbf{p}, z=L)\rangle = \langle u(\mathbf{p})u^*(\mathbf{p})\rangle\\ &= \frac{\left(\frac{k\alpha_s}{2L}\right)^2}{\left(\frac{1}{4\alpha_s^2}+\frac{1}{\rho_0^2}+\frac{k^2\alpha_s^2}{4L^2}\right)}\exp\left[-\frac{\left(\frac{k\alpha_s}{L}\right)^2\left(p_x^2+p_y^2\right)}{\left(1+\left(\frac{2\alpha_s}{\rho_0}\right)^2+\left(\frac{k\alpha_s^2}{L}\right)^2\right)}\right]\end{aligned} \tag{6}$$

In Eq. (6), ρ_0 represents the coherence length of a spherical wave as it propagates through the tissue turbulence, and it is defined by the expression [17].

$$\rho_0 = \left[\frac{\pi^2k^2z}{3}\int_0^{\infty}\kappa^3\Phi(\kappa)\mathrm{d}\kappa\right]^{-1/2}, \tag{7}$$

where κ signifies the spatial frequency, $\Phi(\kappa)$ denotes the power spectrum of the biological tissue and is expressed as follows [20,21]

$$\Phi_n(\kappa) = \frac{Sl_c^3\Gamma(D_f/2)}{\pi^{3/2}2^{(5-D_f)/2}\left(1+\kappa^2l_c^2\right)^{D_f/2}}\exp\left(\frac{-\kappa^2l_0^2}{8\ln 2}\right). \tag{8}$$

Here S is the strength coefficient of the refractive-index fluctuations, l_c is the characteristic length of heterogeneity, $\Gamma(.)$ is the gamma function, D_f is the fractal dimension, l_0 is the small length-scale factor. We apply the tissue turbulence power spectrum model from Eq. (8) within Eq. (7) to derive the coherence length of the spherical wave in biological tissue

$$\rho_0 = \left[\frac{1}{3}\sqrt{\pi}k^2L\frac{S}{2^{(7-D_f)/2}l_c}\Gamma\left(\frac{D_f}{2}\right)U\left(2;\frac{6-D_f}{2};\frac{l_0^2}{8\ln(2)l_c^2}\right)\right]^{-1/2}, \tag{9}$$

where $U(.)$ is the confluent hypergeometric function of the second kind. Eq. (9) is derived by employing Equation (2.1) of Belafhal et al. [22] which is

$$\int_0^{\infty}\frac{e^{-\varepsilon t^2}t^{2\mu-1}}{(1+ct^2)^{\upsilon}}dt = \frac{\Gamma(\mu)}{2c^{\mu}}U\left(\mu;\mu+1-\upsilon;\frac{\varepsilon}{c}\right), \mu, c>0, \tag{10}$$

2.2. Average transmittance due to tissue turbulence

The average transmittance of the Gaussian beam, affected by tissue turbulence, has been found on the receiver axis ($\mathbf{p} = 0$) i.e. Strehl ratio which is given by [18]

$$\langle\tau_t\rangle = \frac{\langle I(0,L)\rangle}{I^0(0,L)} \tag{11}$$

where $\langle I(0, L)\rangle$ is the average received on-axis optical intensity in tissue turbulence, $I^0(0,L)$ denotes the received on-axis optical intensity in the absence of turbulence. It is important to note that the average transmittance is within the range of 0 to 1. A value of 1 implies that the optical wave passes through the medium without any distortion, while a value of 0 indicates complete obstruction of the optical wave by the turbulent medium.

2.3. Transmittance due to absorption and scattering

The attenuation in intensity due to absorption and scattering is

calculated by applying the Beer-Lambert Law [23]

$$I = I^0 exp[-c(\lambda)L], \tag{12}$$

where I represents the received on-axis intensity after propagating through the tissue medium, in the presence of scattering and absorption, I^0 is the received on-axis intensity in the absence of absorption and scattering, $c(\lambda) = a(\lambda) + b(\lambda)$ is the total extinction coefficient, $a(\lambda)$ and $b(\lambda)$ being the absorption and the scattering coefficients, respectively. It is important to emphasize that the absorption and scattering coefficients exhibit wavelength dependence and can be directly obtained from the references specified in [1–5], with empirical measurements derived from diverse tissue samples. The transmittance as a result of absorption and scattering $\tau_{a,s}$ can be expressed as

$$\tau_{a,s} = \frac{I}{I^0} = exp[-c(\lambda)L]. \tag{13}$$

2.4. Transmittance due to turbulence, absorption and scattering

The transmittance arising from the combined effects of turbulence, absorption, and scattering $\tau_{t,a,s}$ is calculated by multiplying the average transmittance of light due to turbulence with the transmittance due to absorption and scattering. That is

$$\tau_{t,a,s} = \langle \tau_t \rangle . \tau_{a,s} = \frac{\langle I(0,L) \rangle}{I^0(0,L)} exp[-c(\lambda)L]. \tag{14}$$

In this research, we have gathered tissue parameter data related to turbulence and absorption-scattering from sources [2,3,24] to investigate $\langle \tau_t \rangle$, $\tau_{a,s}$, and $\tau_{t,a,s}$.

3. Numerical results

In this section, we have numerically explored the average transmittance of a light beam as it propagates through tissue media with distinct distortion characteristics, including turbulence, absorption, and scattering. In the following analyses, within Figs. 1–6, we exclusively explore how tissue turbulence impacts the average transmittance across different tissue types. Moving on to Figs. 7 and 9, our focus shifts solely to examining how absorption and scattering affect transmission in various human tissues. Lastly, Figs. 8 and 10 illustrate the impact of absorption, scattering, turbulence, and their combined effect on transmittance.

Fig. 1 illustrates the comparison of average transmittance $\langle \tau_t \rangle$ versus propagation distance L for various biological tissue types. The tissue types compared here are liver parenchyma of mouse having measured parameters D_f =2.60 and $l_C = 10.24\ \mu$m, intestinal epithelium of mouse having measured parameters D_f =2.67 and $l_C = 11.48\ \mu$m, upper dermis of human having measured parameters D_f =2.67 and $l_C = 5.24\ \mu$m, and deep dermis of mouse having measured parameters D_f =2.72 and $l_C = 5.29\ \mu$m. The parameters are extracted from Table 1 of Ref. [24]. It is

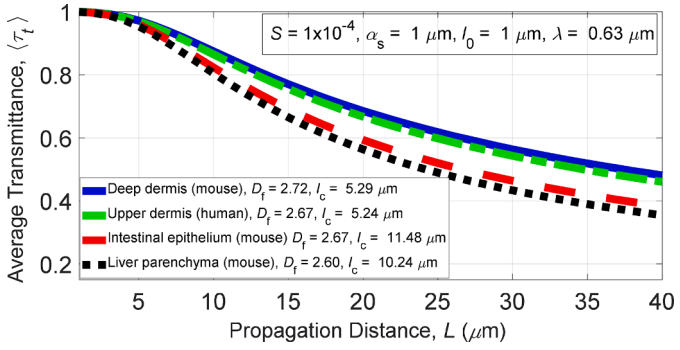

Fig. 1. Average transmittance $\langle \tau_t \rangle$ versus propagation distance L for different tissue types.

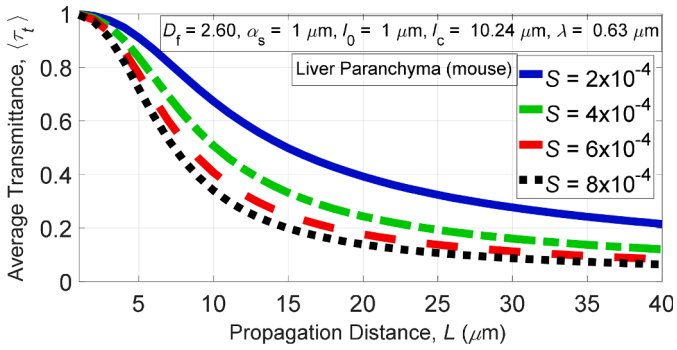

Fig. 2. Average transmittance $\langle \tau_t \rangle$ versus propagation distance L for different S values.

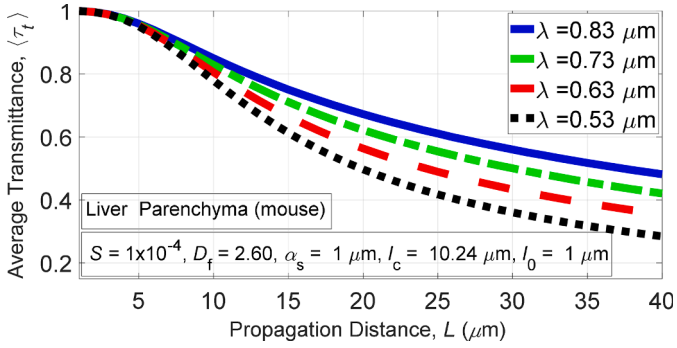

Fig. 3. Average transmittance $\langle \tau_t \rangle$ versus propagation distance L for different wavelength λ values.

seen in Fig. 1 that the average transmittance decreases as the propagation distance increases for all tissue types. At a fixed L value, the maximum transmittance is observed for the tissue named deep dermis (mouse). The average light transmittance of upper dermis (human) is lower than that of deep dermis (mouse). The intestinal epithelium (mouse) has a higher average transmittance than the liver parenchyma (mouse). Notably, liver parenchyma (mouse) shows the least average transmittance among the analyzed tissues. It is crucial to highlight that the deep dermis of mouse and the upper dermis of human tissues demonstrate comparable average transmittance values. Comparable patterns can also be observed between the intestinal epithelium and liver parenchyma of mouse.

In Fig. 2, we depict how the average transmittance of the mouse liver parenchyma is affected by the strength coefficient of refractive-index fluctuations S. This coefficient maintains a constant value of $S = 1 \times 10^{-4}$ as shown in Fig. 1. It is noted that as S increases, there is a decrease in the average transmittance. Fig. 3, akin to Fig. 2, illustrates the relationship between the average transmittance of mouse liver parenchyma and the wavelength of the light source λ. This parameter remains constant at a value of $\lambda = 0.63\mu$m, as depicted in Fig. 1. In Fig. 3, it is evident that with an increase in the wavelength of the light source λ, there is a corresponding increase in the average transmittance. Fig. 4, similar to Figs. 2 and 3, illustrates the correlation between the average transmittance of mouse liver parenchyma and the source size of the Gaussian beam α_s. This parameter is held constant at $\alpha_s = 1\mu$m, as shown in Fig. 1. It is seen that average transmittance increases with increasing the source size of the Gaussian beamα_s.

In Fig. 5, the average transmittance is graphed against the strength coefficient of refractive-index fluctuations S across different characteristic length of heterogeneity l_c values. Similarly, Fig. 6 represents this relationship for various fractal dimension D_f values. We refrain from categorizing l_c and D_f values as they represent characteristics for tissue types. Instead, we consider generic soft tissue types for Figs. 5 and 6. We

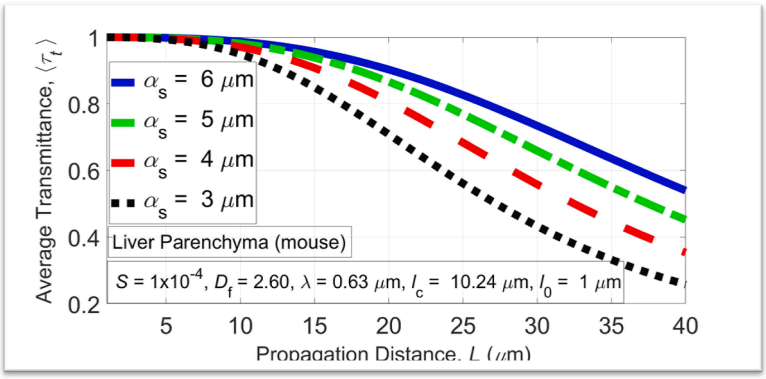

Fig. 4. Average transmittance $\langle\tau_t\rangle$ versus propagation distance L for different source size α_S values.

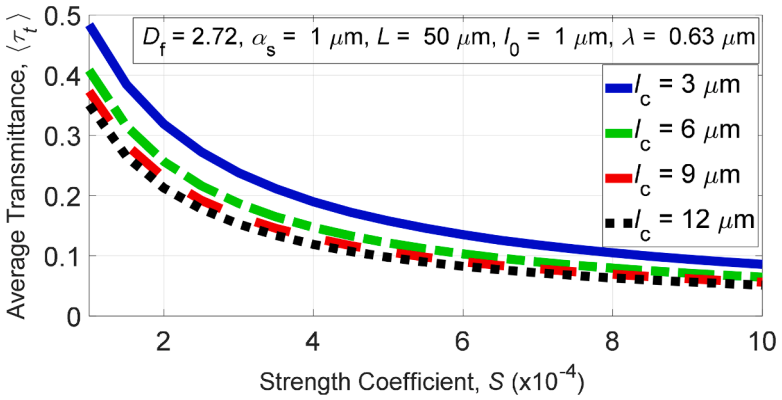

Fig. 5. Average transmittance $\langle\tau_t\rangle$ versus strength coefficient of the refractive-index fluctuations S for different characteristic length of heterogeneity l_c values.

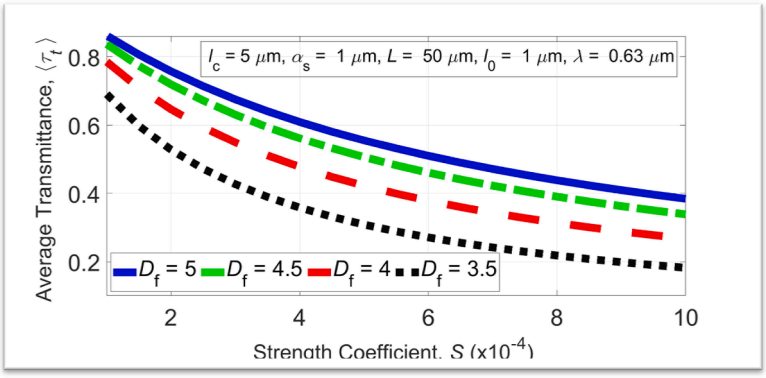

Fig. 6. Average transmittance $\langle\tau_t\rangle$ versus strength coefficient of the refractive-index fluctuations S for different fractal dimension D_f values.

observe in Fig. 5 and 6 that the average transmittance decreases with increasing strength coefficient of the refractive-index fluctuations S values. At a fixed S value in Fig. 5, any rise in characteristic length of heterogeneity l_c leads to a decrease in the average transmittance. It is noteworthy in Fig. 6 that a decrease in the fractal dimension D_f corresponds to a decrease in the average transmittance.

In Fig. 7, the relationship between transmittance and propagation distance across various human tissue types, including dermis, liver, lung, and uterus, is depicted. The data utilized to generate this graph is sourced from Table 1 in [3], which provides absorption and scattering coefficients for these tissues. It is noticeable that as the propagation distance L increases, the transmittance $\tau_{a,s}$ decreases due to absorption and scattering. At a fixed propagation distance of L, the highest level of light transmission is achieved in the human dermis, while the lowest level is observed in the human uterus. Furthermore, human liver tissue exhibits higher light transmission compared to human lung tissue.

In Fig. 8, our objective is to represent the average transmission resulting from turbulence $\langle\tau_t\rangle$, as well as the transmittance resulting from absorption and scattering $\tau_{a,s}$. Moreover, we seek to demonstrate the combined influence of these two factors $\langle\tau_t\rangle.\tau_{a,s}$ on the transmission of the Gaussian beam. In Fig. 8, we first plot the transmittance arising from absorption and scattering $\tau_{a,s}$ for human dermis tissue, as previously shown in Fig. 7 (indicated as a blue solid line). Subsequently, the average transmittance $\langle\tau_t\rangle$ is depicted, employing the characteristic tissue parameters ($D_f = 2.67$ and $l_c = 5.24\mu m$) specific to human dermis extracted from Table 1 of Ref. [24]. It has been discovered that when considering a fixed propagation distance of L, the highest level of transmittance is achieved under the assumption that only turbulence

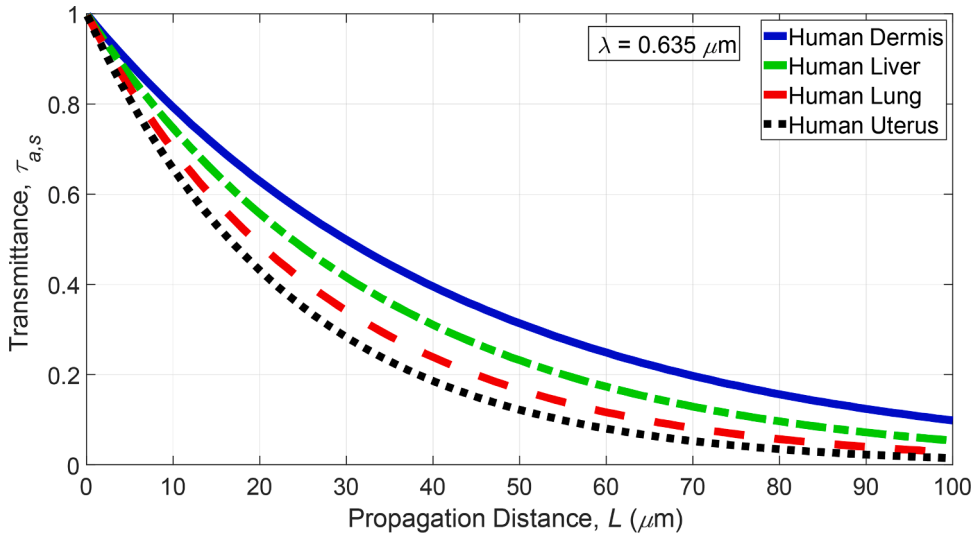

Fig. 7. Transmittance $\tau_{a,s}$ versus propagation distance L across different types of human tissues.

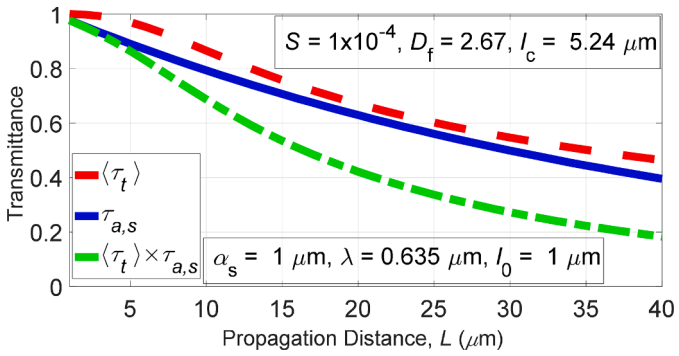

Fig. 8. Transmittance versus propagation distance L across turbulence$\langle\tau_t\rangle$, absorption-scattering $\tau_{a,s}$, and their combined effect$\langle\tau_t\rangle.\tau_{a,s}$ for human dermis.

exists within the human dermis structure. Moreover, when solely absorption and scattering are present within the human dermis tissue, the Gaussian beam transmittance attributed to absorption and scattering $\tau_{a,s}$ surpasses that resulting from turbulence $\langle\tau_t\rangle$. Once the combined impact of absorption-scattering, and turbulence $\langle\tau_t\rangle.\tau_{a,s}$ is taken into consideration, there is a notable decrease in the transmittance of the light wave.

Fig. 9 depicts the relationship between transmittance and propagation distance across different wavelength values for both normal and metastatic human liver tissues. The data necessary for constructing Fig. 9 is sourced from Table 1 of [2], which provides the absorption and scattering coefficients. We observe that as the propagation distance increases the transmittance $\tau_{a,s}$ due to absorption and scattering decreases. For a constant propagation distance L, metastatic human tissue exhibits higher transmittance values in comparison to normal liver tissue. It is notable that changes in wavelength affect transmittance differently for normal and metastatic tissues. Specifically, as the wavelength increases, transmittance rises for normal tissue, whereas the opposite trend is observed for metastatic tissue.

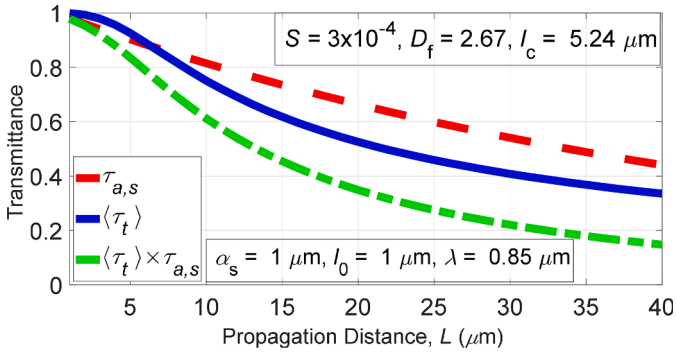

Fig. 10. Transmittance versus propagation distance L across turbulence$\langle\tau_t\rangle$, absorption-scattering $\tau_{a,s}$, and their combined effect$\langle\tau_t\rangle.\tau_{a,s}$.

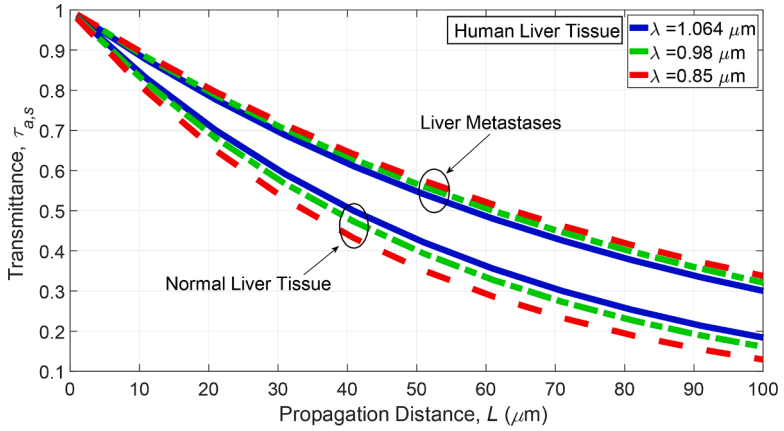

Fig. 9. Transmittance $\tau_{a,s}$ versus propagation distance L for different wavelength λ values.

In Fig. 10, our goal is to illustrate the average transmittance resulting from turbulence $\langle\tau_t\rangle$, as well as the transmittance resulting from absorption and scattering $\tau_{a,s}$. Additionally, we aim to show the combined impact of these two phenomena $\langle\tau_t\rangle.\tau_{a,s}$ on the transmittance of the Gaussian beam. In Fig. 10, we initially plot the transmittance resulting from absorption and scattering $\tau_{a,s}$ for normal human liver tissue, which is also depicted in Fig. 9 for the wavelength of $\lambda = 0.85\ \mu$m (shown as a red dashed line). Unfortunately, the turbulence parameters l_c and D_f specific to normal human liver tissue have not been documented in existing literature. As a substitute, we have selected $D_f = 2.67$ and $l_c = 5.24\mu$m for representation in Fig. 10. It is found that the effect of turbulence on reducing light wave transmittance $\langle\tau_t\rangle$ outweighs that of absorption and scattering $\tau_{a,s}$. When taking into account the combined impact of absorption, scattering, and turbulence $\langle\tau_t\rangle.\tau_{a,s}$, the transmittance of light wave is significantly diminished.

4. Conclusion

In this research, we have examined the transmittance of a Gaussian laser beam that propagates through different biological tissues, including the intestinal epithelium and liver parenchyma of mouse, the upper and deep dermis of human, as well as human liver, lung, and uterus tissues. The medium within these tissue structures displays both turbulence and absorption-scattering effects. By applying the Huygens-Fresnel principle and the Beer-Lambert law, we determine the intensity at the observation point. This intensity is then divided by the intensity in free space to compute the average transmittance. We have found that as the propagation distance L increases, we observed a decrease in transmittance, consistent with our expectations. A decrease in strength coefficient of the refractive-index fluctuations S and the characteristic length of heterogeneity l_c make the average transmittance increase. Further, as the wavelength λ, source size α_s, and the fractal dimension D_f increase, the average transmittance increases. In some cases, absorption and scattering effects $\tau_{a,s}$ can reduce light wave transmittance more significantly than turbulence $\langle\tau_t\rangle$ although the opposite effect is also observed. Considering the combined impact of absorption, scattering, and turbulence $\langle\tau_t\rangle.\tau_{a,s}$, the transmittance of the light wave is prominently reduced.

It is worth noting that examining how light wave behaves in various tissues, as discussed with the Gaussian beam transmittance in this study, offers insights into internal tissue structure. Understanding normal tissue functioning aids in detecting and contrasting abnormal conditions. Thus, further research, especially measuring turbulence and absorption-scattering parameters in tissues, is necessary for improved analyses of the Gaussian beam transmittance. Having this information will also be useful in calculating different entities of the light beam.

CRediT authorship contribution statement

Murat Kaan Özcan: Writing – original draft, Visualization, Software, Resources, Investigation. **Muhsin Caner Gökçe:** Writing – review & editing, Visualization, Methodology. **Yahya Baykal:** Writing – review & editing, Supervision, Investigation, Conceptualization.

Declaration of competing interest

The authors declare that they have no known competing financial interests or personal relationships that could have appeared to influence the work reported in this paper.

Data availability

Data will be made available on request.

References

[1] Jacques SL. Optical properties of biological tissues: a review. Phys Med Biol 2013; 58(11). https://doi.org/10.1088/0031-9155/58/11/R37. May.

[2] Germer CT, Roggan A, Ritz JP, Isbert C, Albrecht D, Müller G, Buhr HJ. Optical properties of native and coagulated human liver tissue and liver metastases in the near infrared range. Lasers Surg Med 1998;23(4):194–203. https://doi.org/10.1002/(sici)1096-9101(1998)23:4<194::aid−lsm2>3.0.co;2-6. Dec.

[3] Marchesini R, Bertoni A, Andreola S, Melloni E, Sichirollo AE. Extinction and absorption coefficients and scattering phase functions of human tissues *in vitro*. Appl Opt 1989;28(12):2318–24. https://doi.org/10.1364/AO.28.002318. June.

[4] Rastegar S, Jacques SL, Motamedi M, Kim BM. Theoretical analysis of equivalency of high-power diode laser (810nm) and Nd:YAG laser (1064nm) for coagulation of tissue: predictions for prostate coagulation. SPIE Proc Laser Tissue Interaction III 1992;1646. https://doi.org/10.1117/12.137454.

[5] Hillegersberg RV, Pickering JW, Aalders M, Beek JF. Optical properties of rat liver and tumor at 633 nm and 1064 nm: photofrin enhances scattering. Lasers Surg Med 1993;13(1):31–9. https://doi.org/10.1002/lsm.1900130108.

[6] Gökçe MC, Ata Y, Baykal Y. Tissue turbulence and its effects on optical waves: a review. Opt Commun 2023;546:129816. https://doi.org/10.1016/j.optcom.2023.129816. article numberNov.

[7] Gökçe MC, Baykal Y. Effects of liver tissue turbulence on propagation of annular beam. Optik 2018;171:313–8. https://doi.org/10.1016/j.ijleo.2018.06.058 (Stuttg)Sept.

[8] Gökçe MC, Baykal Y, Ata Y. Laser array beam propagation through liver tissue. J Vis 2020;23:331–8. https://doi.org/10.1007/s12650-020-00630-5 (Tokyo)Feb.

[9] Luo M, Chen Q, Hua L, Zhao D. Propagation of stochastic electromagnetic vortex beams through the turbulent biological tissues. Phys Lett A 2014;378(3):308–14. https://doi.org/10.1016/j.physleta.2013.11.022. Jan.

[10] Lu X, Zhu X, Wang K, Zhao C, Cai Y. Effects of biological tissues on the propagation properties of anomalous hollow beams. Optik 2016;127(4):1842–7. https://doi.org/10.1016/j.ijleo.2015.11.039 (Stuttg).

[11] Ebrahim AAA, Belafhal A. Effect of the turbulent biological tissues on the propagation properties of Coherent Laguerre-Gaussian beams. Opt Quantum Electron 2021;53(4):179. https://doi.org/10.1007/s11082-021-02838-7. article numberMarch.

[12] Saad F, Benzehoua H, Belafhal A. Analysis on the propagation characteristics of a Generalized Hermite cosh-Gaussian beam through human upper dermis tissue. Opt Quantum Electron 2024;56. https://doi.org/10.1007/s11082-023-06259-6. article number 599Jan.

[13] Baykal Y, Arpali Ç, Arpali SA. Scintillation index of optical spherical wave propagating through biological tissue. J Mod Opt 2016;64(2):138–42. https://doi.org/10.1080/09500340.2016.1214760. July.

[14] Jin H, Zheng W, Ma H, Zhao Y. Average intensity and scintillation of light in a turbulent biological tissue. Optik 2016;127(20):9813–20. https://doi.org/10.1016/j.ijleo.2016.07.077 (Stuttg)Oct.

[15] Chen X, Li J, Korotkova O. Light scintillation in soft biological tissues. Waves Random Complex Media 2020;30(3):481–9. https://doi.org/10.1080/17455030.2018.1530814.

[16] Ata Y, Gökçe MC, Baykal Y. Intensity fluctuations in biological tissues at any turbulence strength. Phys Scr 2022;97(9):095501. https://doi.org/10.1088/1402-4896/ac83f7. Aug.

[17] Andrews LC, Philips RL. Laser beam propagation through random media. 2nd ed. Bellingham, WA, USA: SPIE; 2005.

[18] Gökçe MC, Baykal Y, Ata Y, Gerçekcioğlu H. Multimode beam propagation through atmospheric turbulence. J Quant Spectrosc Radiat Transf 2024;314:108857. https://doi.org/10.1016/j.jqsrt.2023.108857. article numberFeb.

[19] Wang SJ, Baykal Y, Plonus MA. Receiver-aperture averaging effects for the intensity fluctuation of a beam wave in the turbulent atmosphere. J Opt Soc Am 1983;73(6):831–7. https://doi.org/10.1364/JOSA.73.000831. June.

[20] Radosevich AJ, Yi J, Rogers JD, Backman V. Structural length-scale sensitivities of reflectance measurements in continuous random media under the Born approximation. Opt Lett 2012;37(24):5220–2. https://doi.org/10.1364/OL.37.005220. Dec.

[21] Liang Q, Hu B, Zhang Y, Zhu Y, Deng S, Yu L. Coupling efficiency of a partially coherent collimating laser from turbulent biological tissue to fiber. Results Phys 2019;13:102162. https://doi.org/10.1016/j.rinp.2019.102162. article numberJune.

[22] Belafhal A, Chib S, Khannous F, Usman T. Evaluation of integral transforms using special functions with applications to biological tissues. Comput Appl Math 2021; 40:156. https://doi.org/10.1007/s40314-021-01542-2. article numberMay.

[23] Oshina I, Spigulis J. Beer–Lambert law for optical tissue diagnostics: current state of the art and the main limitations. J Biomed Opt 2021;26(10):100901. https://doi.org/10.1117/1.JBO.26.10.100901. Oct.

[24] Schmitt JM, Kumar G. Turbulent nature of refractive-index variations in biological tissue. Opt Lett 1996;21(16):1310–2. https://doi.org/10.1364/OL.21.001310. Aug.